Stress analysis of GaN-based heterostructures on silicon substrates

© *D.S. Arteev*[1], *A.V. Sakharov*[1], *E.E. Zavarin*[1], *A.E. Nikolaev*[1], *M.A. Yagovkina*[1], *A.F. Tsatsulnikov*[2]

[1] Ioffe Institute,
194021 St. Petersburg, Russia
[2] Submicron Heterostructures for Microelectronics, Research & Engineering Center,
Russian Academy of Sciences,
194021 St. Petersburg, Russia

E-mail: ArteevDS@mail.ioffe.ru

Elastic stresses in AlN layers on silicon substrates of different thickness, as well as in multilayer (Al, Ga)N structures grown on AlN/Si templates, were investigated based on in-situ reflectometry/deflectometry data. It was found that tensile stresses arise during the growth of AlN, with their magnitude increasing with thicker the substrate. During the growth of multilayer step-graded (Al, Ga)N structures, all layers underwent compressive stress which decreased towards the surface. After cooling the structures to room temperature, some of the lower AlGaN layers remained entirely compressed, while another part experienced both compressive (in the lower part of each layer) and tensile (in the upper part of each layer) stresses

High electron mobility transistors based on III-V compounds are increasingly becoming part of modern electronics, gradually replacing existing silicon-based devices. Gallium nitride has a unique combination of properties, such as a large band gap (3.4 eV, 3 times that of silicon), high electron saturation velocity ($\sim 2.5 \cdot 10^7$ cm/s) [1], high breakdown electric field strength (> 3 MV/cm) [2] and relatively high mobility (~ 2500 cm^2/(V·s)) of the two-dimensional electron gas at the Al(Ga)N/GaN [3] heterointerface. Due to these properties, it is possible to create high-power [4] and high-frequency [5] devices based on III-N heterostructures.

Due to the lack of inexpensive large-diameter GaN substrates, most III-N-based structures are grown heteroepitaxially on silicon carbide or sapphire substrates. Growth is also possible on silicon substrates, which offer several advantages, namely much lower cost, relatively good thermal conductivity, and commercial availability of substrates up to 450 mm [6] in diameter. However, a serious disadvantage of these substrates is the large lattice mismatch between silicon and III-N compounds, as well as the large difference in the thermal expansion coefficient (TEC), which leads to high dislocation density and cracking of the grown structure during cooling from the epitaxial growth temperature ($\sim 1000°$C for GaN growth by vapor-phase epitaxy and $600-800°$C for growth by molecular-beam epitaxy) to room temperature and limits the maximum possible thickness of the GaN layer. One way to overcome this limitation is to use AlGaN transition buffer layers of different composition [7].

This work presents the results of the analysis of elastic stresses arising during the growth of III-N layers on Si(111) silicon substrates.

The studied structures were grown by metalorganic vapor-phase epitaxy in Dragon-125 system with a horizontal reactor. The system is equipped with a laser reflectometry/deflectometry tool that allows *in situ* control of the layer growth rate and changes in the curvature of the structure. Trimethylgallium, trimethylaluminium and ammonia were used as precursors. Ferrocene and propane were used as iron and carbon doping sources, respectively. Hydrogen, nitrogen and their mixtures acted as carrier gases.

First, a set of templates were grown, which were ~ 215 nm layers of AlN on silicon substrates of varying thicknesses. Growth occurred at a temperature of 1100°C. The values of elastic stresses σ_f in the layers were determined using the Stoney equation:

$$\kappa = \frac{6 M_f \varepsilon_f h_f}{M_s h_s^2} = \frac{6 \sigma_f h_f}{M_s h_s^2}, \quad (1)$$

where κ — curvature, $M_{f,(s)}$ — biaxial elastic modulus, $h_{f,(s)}$ — layer (substrate) thickness, where $h_f = G_f t$, where G_f — layer growth rate. Hereinafter, the values of all necessary parameters were taken from [8]. On the other hand, the stress caused by the mismatch of lattice constants a, can be written as $\varepsilon_f = (a_s - a_f)/a_s(1 - r)$, where r — the degree of plastic relaxation. The change in curvature during the growth of the AlN layer for samples grown on substrates with thicknesses of 950, 685, 500 μm is shown in Figure 1, *a*. The obtained values of elastic stress σ_f and relaxation degree r of AlN layers grown on substrates of different thicknesses are shown in Figure 1, *b*. It can be seen that the magnitude of the tensile stress is larger the thicker the substrate, while the degree of relaxation, on the contrary, is smaller. For the AlN layer grown on a 500 μm thick substrate, the elastic stress is 1.02 GPa, which
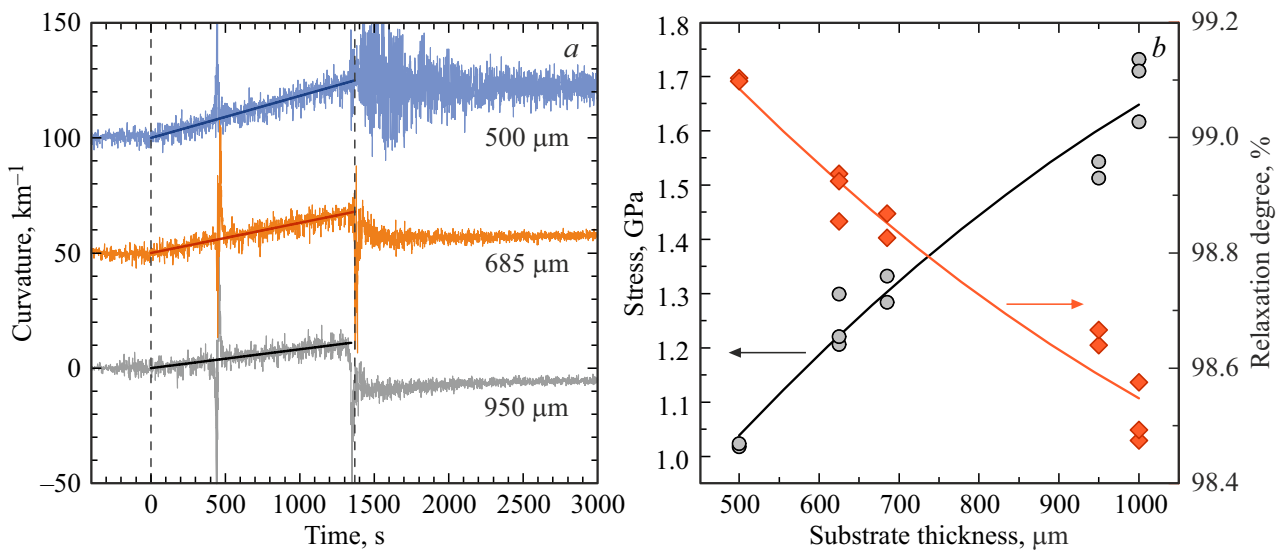
Figure 1. *a* — changes in substrate curvature during the growth of AlN layer on silicon substrates with thicknesses of 950, 685, and 500 μm. Dependencies are shifted vertically for clarity. The dashed vertical lines indicate the beginning and the end of the layer growth process. *b* — the dependence of the elastic stresses and the degree of plastic relaxation of the AlN layer on the substrate thickness.

agrees well with the value ~ 1.2 GPa from [9] for a layer grown on a silicon substrate of the same thickness under similar growth conditions. It was also reported in [10] that the stress value in an AlN layer grown by molecular-beam epitaxy on a 300 μm-thick substrate was $0.5 - 0.7$ GPa. The generation of such tensile stress is attributed to the coalescence of islands in the layer growing by the Volmer–Weber [11,12] mechanism. However, the reflectometry data show no evidence of island growth, so if it does occur, it is only in the very early stages of growth, and the resolution of our equipment (at this growth rate) does not allow us to observe this effect. The reason for the dependence of the stress on substrate thickness is also unclear.

Multilayer (Al, Ga)N structures were grown on these AlN/Si templates. First, six AlGaN layers (AlGaN1, AlGaN2, ..., AlGaN6) with a step-graded Al mole fraction (0.76/0.62/0.40/0.29/0.14/0.06) doped with iron were deposited at 1050°C. To improve the morphology, the layers were co-doped with carbon [13]. Then, the growth of GaN : Fe, C (LT-GaN) buffer layer took place at the same temperature. Afterwards, a high temperature undoped GaN layer (HT-GaN) was deposited at 1100°C. Iron-doped buffer layers are widely used in GaN-based high electron mobility transistors; the optimally selected thickness of the undoped layer (channel) makes it possible to obtain high breakdown voltages without significant deterioration of the properties of the two-dimensional electron gas caused by the penetration of iron atoms into the channel region due to the so-called „memory effect" [14,15]. Growth conditions are described in more detail in [16]. Figure 2 shows the X-ray diffraction rocking curve analysis of such a multilayer structure, on which eight separate peaks corresponding to layers of different compositions are clearly distinguishable.
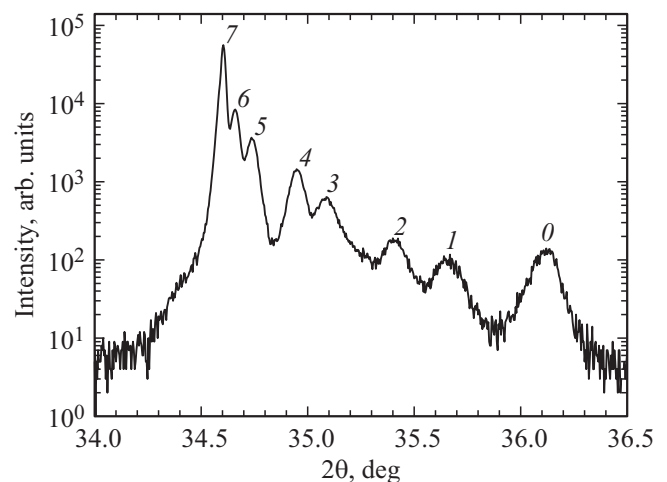
Figure 2. X-ray rocking curve of a multilayer (Al, Ga)N structure. The peaks correspond to the layers: *0* — AlN; *1, 2, . . ., 6* — AlGaN1, AlGaN2, . . ., AlGaN6; *7* — GaN.

The curvature change dependences of the structures during growth on AlN/Si templates grown on substrates with thicknesses of 950 and 685 μm are shown in Figure 3, *a* (in the growth process on a thinner template on a substrate of 500 μm there was plastic deformation of silicon, so this structure was not analyzed and is not shown here). Similar to the growth of AlN layers, a larger curvature change is observed for the growth on the thinner template. However, within each individual layer, the change in curvature is non-linear in time (i.e., layer thickness), so an approach from [17] was used to analyze these structures by approximating the change in curvature of the structure within each layer by a quadratic function $\kappa = A + B_1 h_f + B_2 h_f^2$. Then
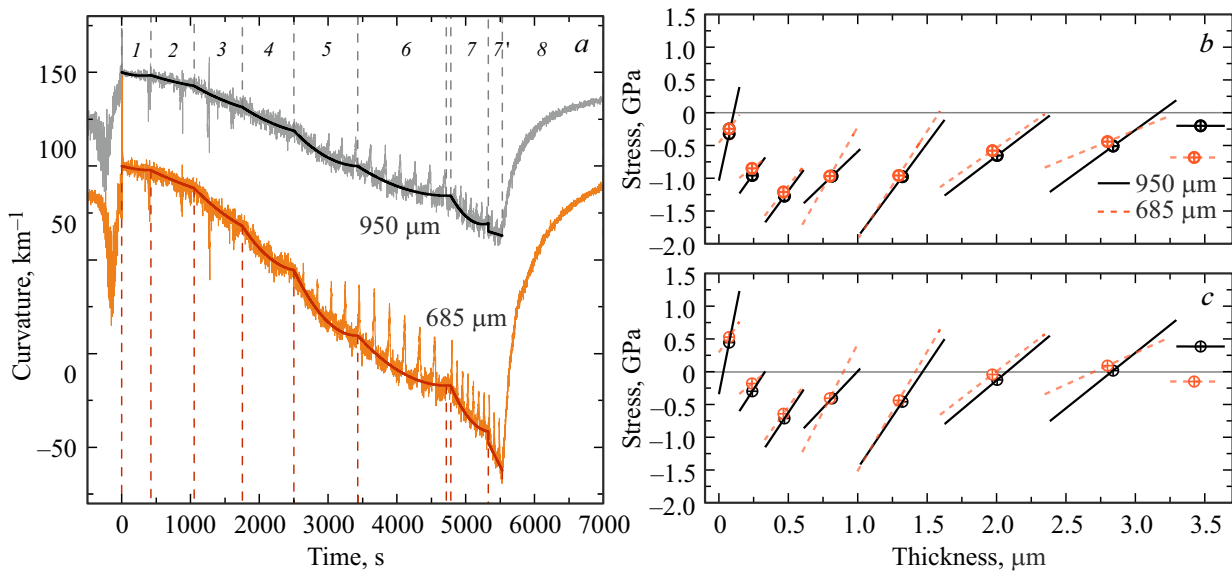
Figure 3. *a* — change in curvature of heterostructures during growth on AlN/Si-templates grown on substrates with thicknesses of 950 and 685 μm Dependencies are shifted vertically for clarity. The dashed vertical lines indicate the beginning and end of the growth process of individual layers: *1, 2, . . ., 6* — AlGaN1, AlGaN2, . . ., AlGaN6; *7* and *7′* — LT-GaN and HT-GaN; *8* — post-growth cooling. *b* — elastic stress distribution along the thickness at the growth temperature. *c* — thickness elastic stress distribution after cooling to room temperature. (The colored version of the figure is available on-line).

the elastic stress distributions in each layer are expressed as

$$\sigma_f(h_f) = \frac{M_s h_s^2}{6} B_1 + \frac{M_s h_s^2}{3} h_f B_2 + \frac{h_s h_f (2M_f - M_s)}{3} B_1. \quad (2)$$

The curves approximated by the quadratic function are also shown in Figure 3, *a*. The calculated elastic stress distribution in the layers at growth temperatures is shown in Figure 3, *b*. Symbols indicate the average stress values within each layer. In the growth process, all layers are almost completely in the compressed state, and as the layer grows, its gradual relaxation occurs, i.e., the part of the layer closer to the surface becomes less stressed (up to an almost stress-free state for low-composition AlGaN5 and AlGaN6 layers and LT-GaN). Stress relaxation occurs by annihilation and tilting of dislocations [18]. On average, the layers on the thinner template are in a slightly less stressed state, although the difference between the structures is not significant. The only exception is the top HT-GaN layer, which is significantly more compressed in the structure grown on the thinner template.

As mentioned above, silicon and III-N materials have very different TECs, which leads to the generation of additional elastic stress during the post-cooling of the structure. In the zero-order approximation, the total elastic stress at room temperature in each layer can be calculated as

$$\sigma_f(T_{RT}) = \sigma_f(T_{\text{growth}}) + M_f \int\limits_{T_{\text{growth}}}^{T_{RT}} [\alpha_s(T) - \alpha_f(T)] dT, \quad (3)$$

where $\alpha_{f,(s)}$ — TEC of the layer (substrate). It can be seen from Figure 3, *c* that after cooling, the AlGaN1 layer

is tensile on average, the intermediate layers of AlGaN2, AlGaN3, AlGaN4 and AlGaN5 remain in a compressed state, and AlGaN6 and LT-GaN are almost stress-free. It is interesting that the HT-GaN layer is tensile in the structure on the thick template, while it is slightly compressed in the structure on the thin template. In addition, separate regions experiencing tensile strain are observed in almost all layers, which is consistent with calculations of the elastic stress distribution in nominally compressed GaN on AlGaN [19]. This could potentially lead to cracking of the structure after some time, so careful optimization of compositions and thicknesses of transition layers AlGaN is necessary to obtain reliable and durable devices based on such heterostructures.

Thus, in this work, the elastic stress in AlN layers during growth on silicon substrates of different thicknesses, as well as during growth of AlGaN multilayer buffer layers of variable composition on the obtained AlN/Si templates, were investigated using *in situ* laser reflectometry/deflectometry data. It is found that AlN layers experience tensile stress during the growth process. The resulting tensile stress is greater the thicker the substrate. During the growth process of a multilayer step-graded (Al,Ga)N structure, all layers experience compressive stress, which decrease towards to the surface. This indicates the relaxation of compressive stress by tilting and changing the dislocation density. No significant difference in the magnitude of elastic stress of layers grown on thick and thin templates is observed, except for the last high-temperature GaN layer. After cooling the structures from the growth temperature to room temperature, a part of the lower AlGaN layers remains entirely compressed, while another part experiences both

compressive stress (at the bottom of the layer) and tensile stress (at the top of the layer). Such stress distribution could potentially lead to cracking of the structure after some time, so careful optimization of compositions and thicknesses of AlGaN transition layers is necessary to obtain reliable and durable devices based on such heterostructures.

Conflict of interest

The authors declare that they have no conflict of interest.

References

[1] J. Khurgin, Y.J. Ding, D. Jena. Appl. Phys. Lett., **91**, 252104 (2007). DOI: 10.1063/1.2824872

[2] V.A. Dmitriev, K.G. Irvine, C.H. Carter, N.I. Kuznetsov, E.V. Kalinina. Appl. Phys. Lett., **68**, 229 (1996). DOI: 10.1063/1.116469

[3] L. Yang, X. Wang, T. Wang, J. Wang, W. Zhang, P. Quach, P. Wang, F. Liu, D. Li, L. Chen, S. Liu, J. Wei, X. Yang, F. Xu, N. Tang, W. Tan, J. Zhang, W. Ge, X. Wu, C. Zhang, B. Shen. Adv. Funct. Mater., **30**, 2004450 (2020). DOI: 10.1002/adfm.202004450

[4] C.-T. Ma, Z.-H. Gu. Electronics, **8**, 1401 (2019). DOI: 10.3390/electronics8121401

[5] M. Haziq, S. Falina, A.A. Manaf, H. Kawarada, M. Syamsul. Micromachines, **13**, 2133 (2022). DOI: 10.3390/mi13122133

[6] Silicon Wafer 18inch Double Sided Polish P110 $1 \sim 50\Omega$. URL: https://www.fuledalink.com/products/18inch-silicon-wafer-dsp (accessed May 16, 2023).

[7] S. Tripathy, V.K.X. Lin, S.B. Dolmanan, J.P.Y. Tan, R.S. Kajen, L.K. Bera, S.L. Teo, M.K. Kumar, S. Arulkumaran, G.I. Ng, S. Vicknesh, S. Todd, W.Z. Wang, G.Q. Lo, H. Li, D. Lee, S. Han. Appl. Phys. Lett., **101**, 082110 (2012). DOI: 10.1063/1.4746751

[8] Y. Dai, S. Li, H. Gao, W. Wang, Q. Sun, Q. Peng, C. Gui, Z. Qian, S. Liu. J. Mater. Sci. Mater. Electron., **27**, 2004 (2016). DOI: 10.1007/s10854-015-3984-1

[9] S. Raghavan, J.M. Redwing. J. Cryst. Growth, **261**, 294 (2004). DOI: 10.1016/j.jcrysgro.2003.11.020

[10] D.S. Zolotukhin, D.V. Nechaev, S.V. Ivanov, V.N. Zhmerik. Techn. Phys. Lett., **43**, 262 (2017). DOI: 10.1134/S1063785017030130

[11] J.A. Floro, E. Chason, R.C. Cammarata, D.J. Srolovitz. MRS Bulletin, **27**, 19 (2002). DOI: 10.1557/mrs2002.15

[12] B.W. Sheldon, A. Rajamani, A. Bhandari, E. Chason, S.K. Hong, R. Beresford. J. Appl. Phys., **98**, 043509 (2005). DOI: 10.1063/1.1994944

[13] W.V. Lundin, A.V. Sakharov, E.E. Zavarin, D.A. Zakheim, E.Y. Lundina, P.N. Brunkov, A.F. Tsatsulnikov. Pis'ma ZhTF, **45**, 36 (2019). (in Russian). DOI: 10.21883/PJTF.2019.14.48022.17738

[14] D.S. Arteev, A.V. Sakharov, W.V. Lundin, E.E. Zavarin, D.A. Zakheim, A.F. Tsatsulnikov, M.I. Gindina, P.N. Brunkov. J. Phys.: Conf. Ser., **1697**, 012206 (2020). DOI: 10.1088/1742-6596/1697/1/012206

[15] D.S. Arteev, A.V. Sakharov, W.V. Lundin, E.E. Zavarin, A.E. Nikolaev, A.F. Tsatsulnikov, V.M. Ustinov. Materials, **15**, 8945 (2022). DOI: 10.3390/ma15248945

[16] A.V. Sakharov, D.S. Arteev, E.E. Zavarin, A.E. Nikolaev, W.V. Lundin, N.D. Prasolov, M.A. Yagovkina, A.F. Tsatsulnikov, S.D. Fedotov, E.M. Sokolov, V.N. Statsenko. Materials, **16**, 4265 (2023). DOI: 10.3390/ma16124265

[17] A. Krost, A. Dadgar, G. Strassburger, R. Clos. Phys. Status Solidi A, **200**, 26 (2003). DOI: 10.1002/pssa.200303428

[18] S. Raghavan, I.C. Manning, X. Weng, J.M. Redwing. J. Cryst. Growth, **359**, 35 (2012). DOI: 10.1016/j.jcrysgro.2012.08.020

[19] M.E. Rudinsky, E.V. Yakovlev, W.V. Lundin, A.V. Sakharov, E.E. Zavarin, A.F. Tsatsulnikov, L.E. Velikovskiy. Phys. Status Solidi A, **213**, 2759 (2016). DOI: 10.1002/pssa.201600210

Translated by Ego Translating